

## A Simple And Efficient FEM-Implementation Of The Modified Mohr-Coulomb Criterion

Clausen, Johan Christian; Damkilde, Lars

*Published in:*

Proceedings of the 19th Nordic Seminar on Computational Mechanics

*Publication date:*  
2006

*Document Version*

Publisher's PDF, also known as Version of record

[Link to publication from Aalborg University](#)

*Citation for published version (APA):*

Clausen, J. C., & Damkilde, L. (2006). A Simple And Efficient FEM-Implementation Of The Modified Mohr-Coulomb Criterion. In O. Dahlblom, L. Fuchs, K. Persson, M. Ristinmaa, G. Sandberg, & I. Svensson (Eds.), *Proceedings of the 19th Nordic Seminar on Computational Mechanics* (pp. 214-219). Lund Universitet.

### General rights

Copyright and moral rights for the publications made accessible in the public portal are retained by the authors and/or other copyright owners and it is a condition of accessing publications that users recognise and abide by the legal requirements associated with these rights.

- Users may download and print one copy of any publication from the public portal for the purpose of private study or research.
- You may not further distribute the material or use it for any profit-making activity or commercial gain
- You may freely distribute the URL identifying the publication in the public portal -

### Take down policy

If you believe that this document breaches copyright please contact us at [vbn@aub.aau.dk](mailto:vbn@aub.aau.dk) providing details, and we will remove access to the work immediately and investigate your claim.

# A simple and efficient FEM-implementation of the Modified Mohr-Coulomb criterion

Johan Clausen and Lars Damkilde

Esbjerg Institute of Technology  
Aalborg University Esbjerg, Esbjerg, Denmark  
e-mail: jc@aaue.dk and ld@aaue.dk

**Summary** This paper presents a conceptually simple finite element implementation of the combined elasto-plastic Mohr-Coulomb and Rankine material models, also known as Modified Mohr-Coulomb plasticity. The stress update is based on a return mapping scheme where all manipulations are carried out in principal stress space which simplifies the calculations. The model supports both associated and non-associated perfect plasticity.

## Introduction

Materials such as sand and concrete show pressure dependent strength properties. The simplest material model which incorporates this pressure dependency is the Mohr-Coulomb material model. The yield criterion uses the well known parameters friction angle,  $\varphi$ , and cohesion,  $c$

$$f_{MC} = k\sigma_1 - \sigma_3 - \sigma_c = 0, \quad \text{with} \quad k = \frac{1 + \sin \varphi}{1 - \sin \varphi} \quad \text{and} \quad \sigma_c = 2c\sqrt{k} \quad (1)$$

where  $\sigma_1$ ,  $\sigma_2$  and  $\sigma_3$  are the principal stresses. In this paper tension is taken as positive.

When  $c > 0$  the Mohr-Coulomb model predicts a tensile strength which is larger than the tensile strength observed experimentally, see e.g. references [1], [2] and [3]. This discrepancy can be mended by the introduction of the Rankine or "tension cut-off" criterion

$$f_R = \sigma_1 - \sigma_t = 0 \quad (2)$$

where  $\sigma_t$  is the "tension cut-off" value, which is the highest tensile stress allowed in the material. The combination of these criteria is usually referred to as the Modified Mohr-Coulomb Criterion, cf. [2]. On Fig. 1 this criterion can be seen in the principal stress space and in the  $\sigma_1 - \sigma_3$  plane. The Rankine part of the criterion, Eq. (2), is taken to be associated whereas the Mohr-Coulomb part is non-associated.

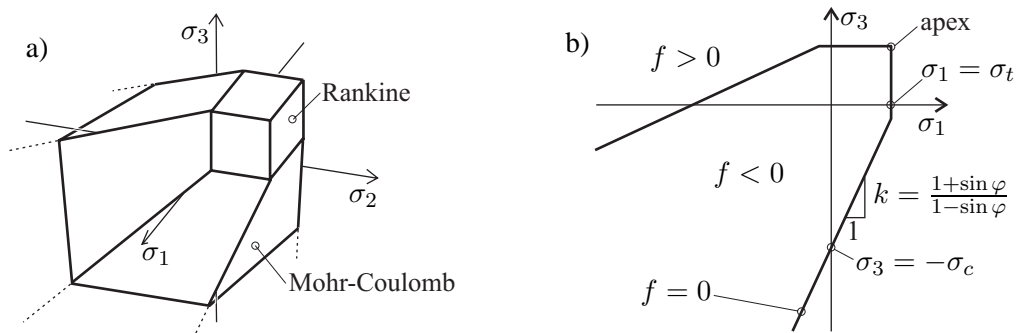


Figure 1: The Modified Mohr-Coulomb Criterion in a) principal stress space and b) the section through the  $\sigma_1 - \sigma_3$  plane.

### Plastic stress update for yield planes in principal stress space

From Eqs. (1), (2) and Fig. 1 it can be seen that the criterion consists of intersecting planes in the principal stress space. As will be shown later the Modified Mohr-Coulomb criterion leads to nine different types of stress return, which must be properly identified. This can be a cumbersome task in general stress space. Therefore the method of [4] and [5] is very well suited for carrying out the plastic integration and formation of the constitutive matrix. In the following a short summary of the method will be given.

The stress update and formation of the consistent constitutive matrix require the derivative of the yield function and the first and second derivatives of the plastic potential. As only isotropic material models are considered the manipulations can be carried out with respect to any set of coordinate axes. Therefore the predictor stress is transformed into principal stress space and returned to the yield surface. Considering the fact that the stress return preserves the principal directions, the updated stress can then be transformed back into the original coordinate system. This simplifies the manipulations of the return mapping scheme considerably compared to the standard formulation, see, e.g. [6]. There are two reasons for this. Firstly the dimension of the problem reduces from six to three, and secondly, in the three-dimensional stress space the stress states can be visualized graphically, making it possible to apply geometric arguments.

Linear yield criteria in the principal stresses are visualized as planes in principal stress space. These planes intersect in lines and points, making three types of stress returns and constitutive matrices necessary: Return to a yield plane, return to a line, e.g. intersection of two yield planes and finally return to a point, e.g. intersection of three or more yield planes. The three types of return are visualized on Fig. 2.

The formulae for the different returns will be established in the following. The conditions for determining which return is needed will also be established by dividing the stress space into different stress regions.

Vectors and matrices are expressed with respect to the principal axes. This means that the last three components of vectors are always zero and are not be shown as a matter of convenience. Even so all matrices and vectors are six-dimensional.

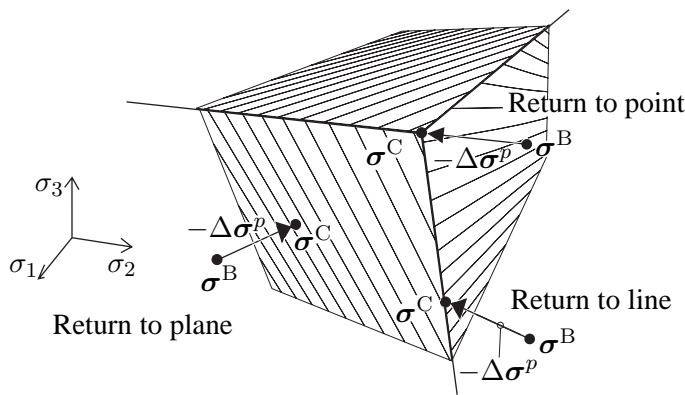


Figure 2: Three intersecting yield planes in principal stress space with three types of return shown.

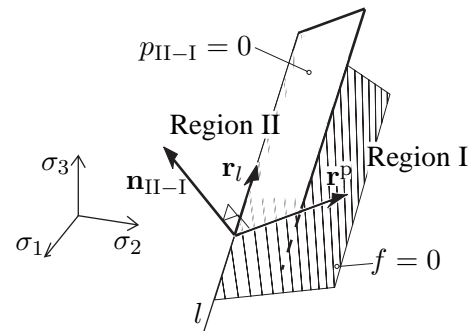


Figure 3: Boundary plane  $p_{II-I} = 0$  with normal  $\mathbf{n}_{II-I}$ , which separates the stress regions I and II.

The task is to determine the updated stress,  $\sigma^C$ , in the equation

$$\sigma^C = \sigma^B - \Delta\sigma^P = \sigma^B - \Delta\lambda \mathbf{D} \frac{\partial g}{\partial \sigma} \quad (3)$$

where  $\sigma^B$  is the predictor stress state found by the solution of the global system of FEM equations,  $\Delta\sigma^P$  is the plastic corrector stress,  $\Delta\lambda$  is a plastic multiplier,  $\mathbf{D}$  is the elastic constitutive matrix and  $g$  is the plastic potential.

#### *Stress return to a plane*

The equation of a yield plane and a plastic potential in the principal stress space can be written as

$$f(\sigma) = \mathbf{a}^T (\sigma - \sigma_f) = 0 \quad \text{and} \quad g(\sigma) = \mathbf{b}^T \sigma \quad (4)$$

where  $\sigma^f$  is a point on the plane and  $\mathbf{a}$  and  $\mathbf{b}$  are the gradients,

$$\mathbf{a} = \frac{\partial f}{\partial \sigma} \quad \text{and} \quad \mathbf{b} = \frac{\partial g}{\partial \sigma} \quad (5)$$

Both  $\mathbf{a}$  and  $\mathbf{b}$  are constant. The plastic corrector stress can be computed as

$$\Delta\sigma^P = \frac{f(\sigma^B)}{\mathbf{b}^T \mathbf{D} \mathbf{a}} \mathbf{D} \mathbf{b} = f(\sigma^B) \mathbf{r}^P \quad \text{with} \quad \mathbf{r}^P = \frac{\mathbf{D} \mathbf{b}}{\mathbf{b}^T \mathbf{D} \mathbf{a}} \quad (6)$$

where  $\mathbf{r}^P$  is the scaled direction of the plastic corrector in principal stress space, i.e.  $\mathbf{r}^P$  is at an angle with the plastic strain direction,  $\mathbf{b}$ .

#### *Stress return to a line*

A line,  $l$ , in principal stress space has the equation

$$l : \sigma = t \mathbf{r}^l + \sigma_l \quad (7)$$

where  $t$  is a parameter with the unit of stress,  $\sigma_l$  is a point on the line and  $\mathbf{r}_l$  is the direction vector. The parameter  $t$  can be found as

$$t = \frac{(\mathbf{r}_1^P \times \mathbf{r}_2^P)^T (\sigma^B - \sigma_l)}{(\mathbf{r}_1^P \times \mathbf{r}_2^P)^T \mathbf{r}_l} \quad (8)$$

where  $\mathbf{r}_1^P$  and  $\mathbf{r}_2^P$  are the plastic corrector vectors from Eq. (6) for the two yield planes intersecting at the line.

#### *Stress return to a point*

If the stress is to be returned to a singularity point,  $\sigma^a$ , e.g. an apex point, see Figure 2, there is no need for calculations, as the returned stress is simply

$$\sigma^C = \sigma^a \quad (9)$$

### Stress regions

In this section it will be outlined how to determine to which plane, line or point the stress should be returned. In order to do this the concept of stress regions is introduced, and the boundary planes that separate them are defined. Each yield plane, line and point is associated with a particular stress region. When the predictor stress is located in a given region it must be returned to the corresponding plane, line or point. Two stress regions, I and II, separated by a boundary plane,  $p_{II-I} = 0$  are illustrated on Figure 3.

When the yield functions and plastic potentials are linear in the principal stresses, the boundary planes are also linear. The direction of the plastic corrector,  $\mathbf{r}^p$ , c.f. (6), and the direction vector of the line,  $\mathbf{r}_l$ , define the orientation of the plane, and so the equation of a boundary plane can be found as:

$$p_{II-I}(\boldsymbol{\sigma}) = (\mathbf{r}^p \times \mathbf{r}_l)^T (\boldsymbol{\sigma} - \boldsymbol{\sigma}_l) = \mathbf{n}_{II-I}^T (\boldsymbol{\sigma} - \boldsymbol{\sigma}_l) = 0 \quad (10)$$

where  $\mathbf{n}_{II-I}$  is the normal of the plane. The indices indicate that the normal points *into* region II *from* region I. The point on the plane is  $\boldsymbol{\sigma}_l$ , which can be taken as a point that also belongs to  $l$ , see Fig. 3 and Eq. (7). If two stress regions are located as seen on Fig. 3, the following is valid for a given predictor stress,  $\boldsymbol{\sigma}^B$  located outside the yield locus, i.e.  $f(\boldsymbol{\sigma}^B) > 0$ :

$$\begin{aligned} p_{II-I}(\boldsymbol{\sigma}^B) &\leq 0 \Leftrightarrow \text{Region I} \Leftrightarrow \text{Return to } f = 0 \\ p_{II-I}(\boldsymbol{\sigma}^B) &> 0 \Leftrightarrow \text{Region II} \Leftrightarrow \text{Return to } l \end{aligned} \quad (11)$$

### Constitutive matrix

The consistent constitutive matrix is also formed in principal stress space. Details are given in refs. [4] and [5].

### Modified Mohr-Coulomb plasticity

The principal stresses are ordered in descending order, i.e.  $\sigma_1 \geq \sigma_2 \geq \sigma_3$ . This means that the Modified Mohr-Coulomb criterion consists of only two planes in the principal stress space, see Fig. 4. As can be seen on the figure the geometry of the yield planes is bounded by five lines which

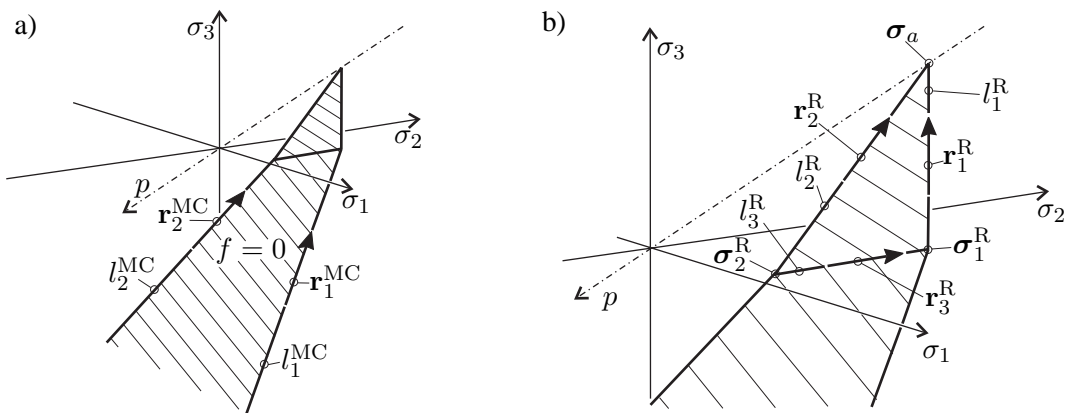


Figure 4: a) The Modified Mohr-Coulomb criterion in principal stress space. b) Detail of the tension cut-off plane,  $f_R$ . The line,  $p$ , is the hydrostatic axis.

intersect at three points. With reference to Fig. 4 the equations for the lines and their direction vectors are

$$l_1^{\text{MC}} : \sigma = t r_1^{\text{MC}} + \sigma_a^{\text{MC}}, \quad \mathbf{r}_1^{\text{MC}} = [1 \ 1 \ k]^T \quad (12)$$

$$l_2^{\text{MC}} : \sigma = t r_2^{\text{MC}} + \sigma_a^{\text{MC}}, \quad \mathbf{r}_2^{\text{MC}} = [1 \ k \ k]^T \quad (13)$$

$$l_1^{\text{R}} : \sigma = t r_1^{\text{R}} + \sigma_a, \quad \mathbf{r}_1^{\text{R}} = [0 \ 0 \ 1]^T \quad (14)$$

$$l_3^{\text{R}} : \sigma = t r_3^{\text{R}} + \sigma_1^{\text{R}}, \quad \mathbf{r}_3^{\text{R}} = [0 \ 1 \ 0]^T \quad (15)$$

where  $t$  is a parameter with the dimension of stress, and  $\sigma_a^{\text{MC}}$ ,  $\sigma_a$  and  $\sigma_1^{\text{R}}$  are the Mohr-Coulomb apex (not shown on Fig. 4), the Modified Mohr-Coulomb apex and the intersection between lines  $l_1^{\text{MC}}$  and  $l_3^{\text{R}}$ , respectively. A fourth point, denoted  $\sigma_1^{\text{R}}$ , is the intersection between lines  $l_2^{\text{MC}}$  and  $l_3^{\text{R}}$ . These points have the coordinates

$$\sigma_a^{\text{MC}} = \frac{\sigma_c}{k-1} \begin{Bmatrix} 1 \\ 1 \\ 1 \end{Bmatrix}, \quad \sigma_a = \begin{Bmatrix} \sigma_t \\ \sigma_t \\ \sigma_t \end{Bmatrix}, \quad \sigma_1^{\text{R}} = \begin{Bmatrix} \sigma_t \\ \sigma_t \\ k\sigma_t - \sigma_c \end{Bmatrix}, \quad \sigma_2^{\text{R}} = \begin{Bmatrix} \sigma_t \\ k\sigma_t - \sigma_c \\ k\sigma_t - \sigma_c \end{Bmatrix} \quad (16)$$

The boundary planes that separate the nine stress regions can be seen on Fig. 5. The equations of the 11 boundary planes will not be given here but can be found from the Eqs. (10) and (12-16).

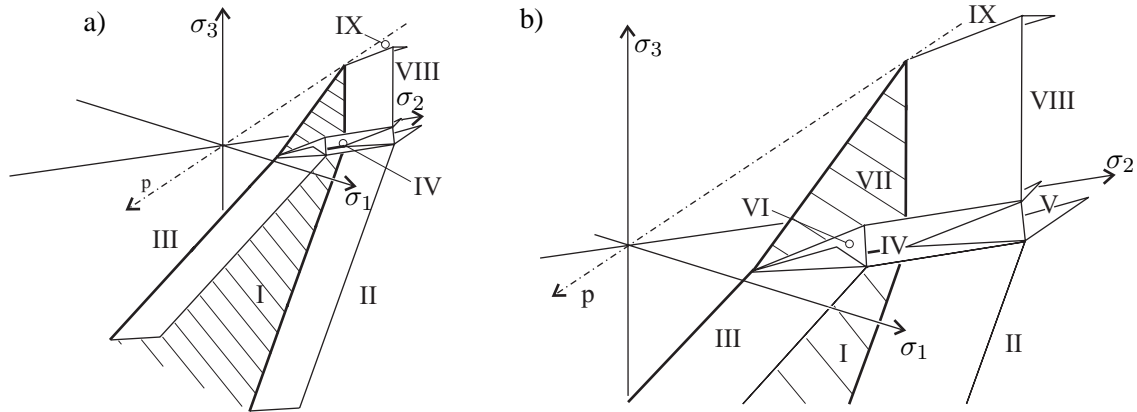


Figure 5: a) Stress regions, denoted by roman numerals. b) Detail.

### Numerical example

A finite element calculation is carried out on a rigid smooth footing resting on a frictional cohesive soil. Two material models are employed. The first is a perfectly plastic Mohr-Coulomb model with  $\varphi = 20^\circ$ ,  $\psi = 5^\circ$  and  $c = 20$  kPa. The second is the Modified Mohr-Coulomb material model with the same parameters and also a tension cut-off,  $\sigma_t = 0$ . A mesh of six-noded triangular linear strain elements is created, and can be seen on Fig. 6. This element mesh has a total of 347 elements with 1500 degrees of freedom. The radius/halfwidth of the footing is  $r$  and the domain has a width of  $12r$  and a height of  $10r$ . A forced displacement is applied to the footing in steps, and the footing pressure  $q$  is found from the reaction forces. The soil has a selfweight of  $\gamma = 20$  kN/m<sup>3</sup>, a modulus of elasticity of  $E = 20$  MPa and a Poisson's ratio of  $\nu = 0.26$ . An initial earth pressure coefficient of  $k_0 = 1$  is used.

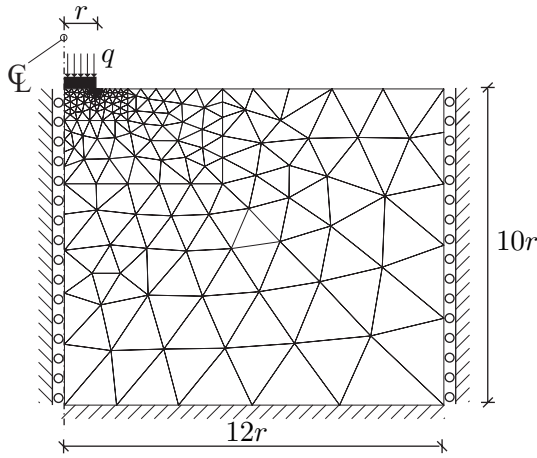


Figure 6: Geometry, boundary conditions and element mesh for the computational example.

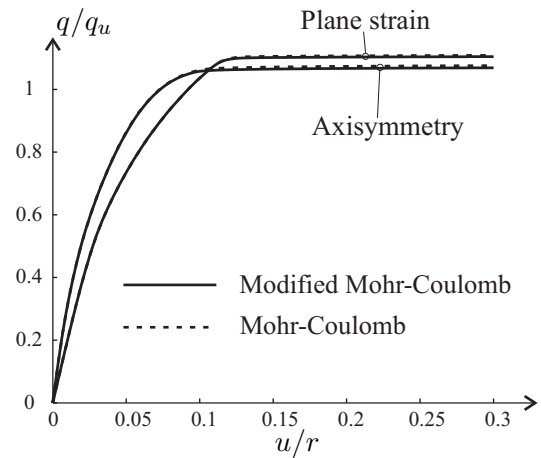


Figure 7: Normalized load-displacement curves.

On Fig. 7 the load-displacement curves can be seen. The displacement has been normalized with respect to the footing radius and the load has been normalized according to Terzaghi's superposition equation for the bearing capacity of surface footings

$$q_u = cN_c + \gamma r N_\gamma \quad (17)$$

Fig. 7 shows that the Mohr-Coulomb and the Modified Mohr-Coulomb model predict almost the same bearing capacity with the Mohr-Coulomb bearing capacity being slightly larger. In a problem with an eccentric load the difference would be more pronounced, as positive normal strains could develop between the soil and a part of the footing without the development of tensile stresses.

## Conclusion

A simple and efficient method of performing the plastic stress update for a Modified Mohr-Coulomb material is presented. In the method all manipulations are carried out in the principal stress space which simplifies these considerably compared to the equivalent manipulations in general six-dimensional stress space. A numerical example shows the performance of the method.

## References

- [1] Mogens Peter Nielsen. *Limit analysis and concrete plasticity*. CRC press, 1999.
- [2] Niels Saabye Ottosen and Matti Ristinmaa. *The Mechanics of Constitutive Modelling*. Elsevier, 2005.
- [3] R.B.J. Brinkgreve and P.A. Vermeer. *Plaxis, Finite Element Code for Soil and Rock Analyses, Version 7*. A.A. Balkema, Rotterdam, 1998.
- [4] Johan Clausen, Lars Damkilde, and Lars Andersen. Efficient return algorithms for associated plasticity with multiple yield planes. *International Journal for Numerical Methods in Engineering*, 66(6):1036–1059, 2006.
- [5] J. Clausen, L. Damkilde, and L. Andersen. An efficient return algorithm for non-associated mohr-coulomb plasticity. In B. H. V. Topping, editor, *Proceedings of the Tenth International Conference on Civil, Structural and Environmental Engineering Computing*, Stirling, United Kingdom, 2005. Civil-Comp Press. paper 144.
- [6] M.A. Crisfield. *Non-Linear Finite Element Analysis of Solids and Structures*, volume 2: Advanced Topics. John Wiley & Sons, 1997.